Tellus
SERIES A
DYNAMIC
METEOROLOGY
AND OCEANOGRAPHY
PUBLISHED BY THE INTERNATIONAL METEOROLOGICAL INSTITUTE IN STOCKHOLM

Tellus (2010), 62A, 647–660

Enhanced evidence in climate models for changes in extratropical atmospheric circulation

By HEIKO PAETH* and FELIX POLLINGER, *Institute of Geography, University of Würzburg, Am Hubland, 97074, Würzburg, Germany*

(Manuscript received 7 October 2009; in final form 11 March 2010)

ABSTRACT

We investigate changes in extratropical atmospheric circulation as derived from the most recent multi-model ensemble of global climate projections. This internationally coordinated systematic data base allows for an accurate assessment of climate change signals against the background of model uncertainty. The multi-model mean time series of the northern-hemisphere (NAM) and southern-hemisphere (SAM) annular modes and of the North Atlantic Oscillation (NAO) are in line with the observed positive trends during the second half of the 20th century and project a further strengthening until the end of the 21st century. For SAM and NAM the simulated changes are unambiguously related to anthropogenic forcing and outperform the level of model uncertainty. This result may imply an enhanced probability for some severe regional impacts of climate change, in particular over extratropical land masses. The climate change signals are noticeably weaker under the B1 mitigation scenario than under the A2 business-as-usual scenario. Ozone forcing has a significant impact on the amplitude of future circulation changes, whereas no systematic effect is found with respect to the models' top-of-the-atmosphere.

1. Introduction

The extent of anthropogenic climate change is often measured by the warming rate of global-mean near-surface temperature (Min and Hense, 2006; IPCC, 2007a). However, for livelihood, mitigation and adaptation strategies the regional dimension of climate change is of larger relevance (IPCC, 2007b). As state-of-the-art global climate models still differ considerably in terms of regional climate change (Tebaldi et al., 2005), the investigation of large-scale circulation modes is an elegant way to get a first glimpse on the regional impacts of global climate change: on the one hand, these leading modes of climate variability are well captured by climate models (Stephenson and Pavan, 2003), on the other hand, they govern a substantial part of regional climate anomalies (Hurrell, 1995; Rauthe and Paeth, 2004; Hurrell et al., 2006; Lubin et al., 2008) and numerous ecological processes (Hallett et al., 2004; Gouveia et al., 2008).

In many regions of the globe, temperature and precipitation variations at the inter-annual to inter-decadal time scale are governed by up to 75% by a few major extratropical circulation modes (Quadrelli and Wallace, 2004; Rauthe and Paeth, 2004). In the Northern Hemisphere, the leading mode of monthly sea level pressure (SLP) variability is the NAM, a ringlike pattern with opposing SLP anomalies over the polar cap and the mid-latitude oceans (Thompson and Wallace, 2001). Its southern-hemisphere counterpart is the SAM (Lubin et al., 2008). In the Atlantic-European sector the NAO represents a more regional mode of variability which is partly in phase with the temporal variations of the NAM and affects climate, environment and society in Eurasia and eastern North America (Hurrell, 1995; Hurrell et al., 2006). In the northern Pacific sector, the Aleutian low, measured by the North Pacific index (NPI), is an important centre of action for regional climate and a modulator for teleconnections associated with the El Niño-Southern Oscillation (Hurrell and van Loon, 1997). The signatures of these leading circulation modes are omnipresent in numerous climatic and ecological variables and, hence, can be regarded as predictors of regional climate impacts due to global warming (Hallett et al., 2004).

Because a strengthening of these circulation modes has been identified in observational data during the second half of the 20th century (Hurrell and van Loon, 1997; Thompson and Wallace, 2001; Marshall, 2003; Hurrell et al., 2006), it has been hypothesized that the circulation changes may be a major indication of the climate's response to enhanced radiative forcing by anthropogenic greenhouse gases (GHG) and aerosols (Deser and Phillips, 2009). As yet the precise mechanism of this response is still a matter of ongoing scientific debate and research

*Corresponding author.
e-mail: heiko.paeth@uni-wuerzburg.de
DOI: 10.1111/j.1600-0870.2010.00455.x

(Rind et al., 2005a,b). On the other hand, as all circulation indices have exhibited multi-decadal fluctuations since preindustrial times, it cannot be ruled out that the observed circulation trends during the second half of the 20th century still represent internal fluctuations (Wunsch, 1999; Paeth et al., 2008; Semenov et al., 2008). Nonetheless, long-term simulations from former climate modelling initiatives mostly draw a picture of further strengthening of the extratropical circulation modes under enhanced greenhouse conditions until 2100 (Ulbrich and Christoph, 1999; Rauthe et al., 2004; Stephenson et al., 2006), implying an additional warming effect over the extratropical land masses and a characteristic pattern of regional precipitation anomalies associated with changes in baroclinic wave activity (Rauthe and Paeth, 2004; Ulbrich et al., 2008). The observed trends are qualitatively consistent with the simulated changes when increasing GHG concentrations are prescribed in the model (Kuzmina et al., 2005; Paeth et al., 2008). However, the models cannot reproduce the observed striking amplitude NAO, NAM and SAM trends as response to GHG forcing (Gillett and Thompson, 2003; Stephenson et al., 2006) but are able to simulate multi-decadal variability similar to what is found in control runs. Miller et al. (2006) have analysed a preliminary subset of the 4th Assessment Report (AR4) data set in terms of changes in the NAM and SAM, particularly in the 20th century. At that time, their limited multi-model ensemble was strongly influenced by the realizations of the GISS model which will be shown to be little representative of the whole AR4 data set meanwhile available.

Some studies have revealed that the changes in extratropical atmospheric circulation may also be sensitive to forcing agents and model setups which are not homogeneously implemented within the AR4 multi-model ensemble. This is particularly true for stratospheric ozone recovery in the 21st century which is taken into account in some of the AR4 climate change simulations and largely affects the direction and amplitude of the circulation changes, in particular, during austral summer in the Southern Hemisphere (Thompson and Solomon, 2002; Miller et al., 2006; Brand et al., 2008; Perlwitz et al., 2008; Son et al., 2008). Therefore, we stress upon the winter changes on both hemispheres when greenhouse forcing probably is the dominant player in extratropical climate change of the Southern Hemisphere as well (Perlwitz et al., 2008). In addition, the vertical resolution (Shindell et al., 1999), the model's top-of-the-atmosphere (TOA) (Gillett et al., 2002; Brand et al., 2008) as well as the correct simulation of stratospheric sudden warmings (Huebener et al., 2007) and stratospheric circulation (Scaife et al., 2005; Dall'Amico et al., 2009) appear to influence the simulated dynamics of extratropical circulation modes.

Motivated by the previous study by Miller et al. (2006), we investigate for the first time the full range of climate model simulations available from the multi-model ensemble of climate projections (Meehl et al., 2007) as realized for the AR4 of the Intergovernmental Panel on Climate Change (IPCC, 2007a,b,c). This model data base is much larger and more systematic than any former international climate modelling initiatives. As an important advancement relative to Miller et al. (2006) and other previous studies the climate change signals in extratropical circulation are quantified, tested and compared with the amount of model uncertainty and internal variability, systematically at different time scales. This type of signal analysis is crucial to assess the confidence decision makers can have in the picture of future climate change as drawn by state-of-the-art climate models. We use a spectral approach to identify the time scale of predictability arising from the radiative forcing (cf. Paeth and Hense, 2004). In addition, we quantify and compare the climate change signals under different emission scenarios to benchmark the potential of mitigation policy with respect to extratropical circulation changes. Finally, we assess the sensitivity of our climate change signals to different stratospheric ozone forcing agents and models' TOA as implemented in the various AR4 climate models.

The following section is dedicated to the considered data sets and statistical methods. The temporal development of the observed and simulated time series for the various circulation indices are presented in Section 3. The climate change signals in the light of model uncertainty and different emission scenarios are assessed in Section 4. The effect of ozone forcing and the models' vertical extent is dealt with in Section 5, whereas the results are summarized and discussed in Section 6.

2. Data and methodology

The observed development of the circulation modes is derived from the Hadley Centre SLP data set (HadSLPr, Allan and Ansell, 2006) during the 1949–2008 period. As previous studies suggested that the SAM trend since the 1950s is considerably overestimated by some SLP data sets due to the lack of station data in the Antarctic (Mo, 2000; Marshall, 2003), we also plot the station-based index by Marshall (2003) which is defined according to the zonal index by Gong and Wang (1999), as a measure of the SAM dynamics in the 20th century.

Model data are taken from the AR4 multi-model ensemble of transient climate change simulations (IPCC, 2007a). This data set consists of ensemble integrations for the 20th and 21st centuries—and partly beyond—from 24 different climate models and under different emission scenarios. During the 20th century all model simulations are driven by observed emission conditions. Table 1 lists the considered model simulations with their specific resolution, stratospheric ozone forcing agent and ensemble size per scenario. Altogether, we account for 133 individual climate change projections. This large model data base represents an excellent starting point to assess climate change signals in the light of model uncertainty and internal model variability (Meehl et al., 2007).

The circulation indices have been computed according to standard definitions based on the monthly SLP field. The NPI is given

Table 1. Considered climate models with horizontal resolution, top-of-the-atmosphere (TOA), stratospheric ozone treatment (O_3), number of ensemble members for the 20th century (20C) as well as for B1, A1B and A2 scenario

Model	Resolution	TOA	O_3	20C	B1	A1B	A2
BCCR-BCM2.0	2.81° × 2.81°	10 hPa	c	1	1	1	1
CCSM3	1,4° × 1.4°	2.2 hPa	r	8	8	7	3
CGCM3.1(T47)	3.75° × 3.75°	1 hPa	c	5	5	5	5
CGCM3.1(T63)	2.81° × 2.81°	1 hPa	c	1	1	1	
CNRM-CM3	2.81° × 2.81°	0.05 hPa	r	1	1	1	1
CSIRO-MK3.0	1.87° × 1.87°	4.5 hPa	r	1	1	1	1
CSIRO-MK3.5	1.87° × 1.87°	4.5 hPa	r	1	1	1	1
ECHAM5/MPI-OM	1.87° × 1.87°	10 hPa	r	4	3	4	3
ECHO-G	3.75° × 3.75°	10 hPa	c	3	3	3	3
FGOALS-g1.0	2.81° × 3°	2.2 hPa	c	3	3	2	
GFDL-CM2.0	2.5° × 2°	3 hPa	r	1	1	1	1
GFDL-CM2.1	2.5° × 2°	3 hPa	r	1	1	1	1
GISS-AOM	4° × 3°	10 hPa	c	2	2	2	
GISS-EH	4° × 3°	0.1 hPa	d	3		3	
GISS-ER	5° × 3.91°	0.1 hPa	d	4	1	3	1
INM-CM3.0	5° × 4°	10 hPa	c	1	1	1	1
INGV-SXG	1.12° × 1.12°	10 hPa	c	1		1	1
IPSL-CM4	3.75° × 2.5°	4 hPa	c	1	1	1	1
MIROC3.2(H)	1.12° × 1.12°	40 km	r	1	1	1	
MIROC3.2(M)	2.81° × 2.81°	30 km	r	3	3	3	3
MRI-CGCM2.3.2	2.81° × 2.81°	0.4 hPa	c	5	5	5	5
PCM	2.81° × 2.81°	2.2 hPa	r	3	1	3	1
UKMO-HadCM3	3.75° × 2.46°	5 hPa	r	1	1	1	1
UKMO-HadGEM1	1.87° × 1.24°	39.2 km	r	1		1	1

Note: Concerning O_3, 'r' means ozone depletion in the 20th century and ozone recovery in the 21st century, 'c' stands for seasonal ozone cycle at pre-industrial level, 'd' denotes ozone depletion in the 20th century and afterwards seasonal ozone cycle at 2000 level, according to IPCC (2007b).

by standardized regional-mean SLP in the sector 30°N to 65°N and 160°E to 140°W (Hurrell and van Loon, 1997). For the index time series of the North Atlantic Oscillation (NAO) SLP pressure is zonally averaged in the sector 10°W to 70°W and 20°N to 70°N and the meridional positions and central pressures of the Icelandic low and Azores high are identified. The NAO index is defined as the leading empirical orthogonal function (EOF) (von Storch and Zwiers, 1999) of these four time series (Rauthe et al., 2004). In contrast to classical static indices, like for instance the pressure gradient between the Lisbon and Iceland (Hurrell and van Loon, 1997), this dynamical NAO index accounts for the meridional displacement of the Atlantic centres of action (Ulbrich and Christoph, 1999). The index of the northern annular mode (NAM) is given by the leading EOF of monthly SLP in the region north of 20°N (Thompson and Wallace, 2001). Accordingly, the index of the southern annular mode (SAM) is the counterpart in the monthly SLP field south of 20°S (Lubin et al., 2008). In the Northern Hemisphere the indices refer to the December to February mean, on the Southern Hemisphere the SAM index is based on the June to August mean, representing the hemispheric winter seasons when the extratropical circulation modes peak (Hurrell and van Loon, 1997; Thompson and Wallace, 2001; Lubin et al., 2008). It has to be noted that the SAM trend during austral summer is more pronounced than during austral winter (Thompson and Solomon, 2002). However, it is supposed that the AR4 multi-model ensemble is more homogeneous in terms of the winter SAM changes when the greenhouse-gas rather than ozone forcing is the dominant impact factor for the SAM dynamics (Perlwitz et al., 2008). For reasons of comparison all index time series – observed and simulated – are normalized to the 1949–2008 period, that is the mean over this period equals zero whereas variability is maintained from each individual data set.

The signal analysis is based on a two-way analysis of variance which uses the systematic bias between different climate models as block effect and the anthropogenic radative forcing as treatment effect (Paeth and Hense, 2002; Wang and Swail, 2006). Given a multi-model ensemble with data x_{ijk} from climate model $i = 1, \ldots, n_i$, run $j = 1, \ldots, n_j$ and time $k = 1, \ldots, n_k$ the quantification of the anthropogenic climate change signal is

based on the linear statistical model

$$x_{ijk} = \mu + \alpha_i + \beta_k + \gamma_{ik} + \varepsilon_{ijk}, \tag{1}$$

where μ is the overall mean of the multi-model ensemble, α_i is the mean over time and all runs from one climate model and represents the systematic difference between climate models, β_k denotes the multi-model ensemble mean time series as a measure of the climate change signal which is common to all model simulations, γ_{ik} corresponds to the ensemble mean time series of each model indicating the different time responses between climate models, and ε_{ijk} is the amount of internal variability which is the unpredictable residual of the statistical model (von Storch and Zwiers, 1999). The individual contributions to total variability of X are determined by square-sum decomposition:

$$SS_t = SS_\alpha + SS_\beta + SS_\gamma + SS_\varepsilon. \tag{2}$$

The sum of squares can be estimated from the data X as follows:

$$SS_\alpha = n_k \sum_{i=1}^{n_i} \left(n_j \, (\bar{x}_{i00} - \hat{\mu})^2\right) \tag{3}$$

$$SS_\beta = n_i n_j \sum_{k=1}^{n_k} (\bar{x}_{00k} - \hat{\mu})^2 \tag{4}$$

$$SS_\gamma = \sum_{i=1}^{n_i} \left(n_i \sum_{k=1}^{n_k} (\bar{x}_{i0k} - \bar{x}_{00k} - \bar{x}_{i00} + \hat{\mu})^2 \right) \tag{5}$$

$$SS_\varepsilon = \sum_{i=1}^{n_i} \sum_{j=1}^{n_j} \sum_{k=1}^{n_k} (x_{ijk} - \bar{x}_{i0k})^2 \tag{6}$$

$$SS_t = \sum_{i=1}^{n_i} \sum_{j=1}^{n_j} \sum_{k=1}^{n_k} (x_{ijk} - \hat{\mu})^2 \tag{7}$$

with

$$\hat{\mu} = \frac{1}{n_i n_j n_k} \sum_{i=1}^{n_i} \sum_{j=1}^{n_j} \sum_{k=1}^{n_k} x_{ijk} \tag{8}$$

$$\bar{x}_{i00} = \frac{1}{n_j n_k} \sum_{j=1}^{n_j} \sum_{k=1}^{n_k} x_{ijk} \tag{9}$$

$$\bar{x}_{00k} = \frac{1}{n_i n_j} \sum_{i=1}^{n_i} \sum_{j=1}^{n_j} x_{ijk} \tag{10}$$

$$\bar{x}_{i0k} = \frac{1}{n_j} \sum_{j=1}^{n_j} x_{ijk} \tag{11}$$

The portion of variance explained by each parameter α_i, β_k γ_{ik} and the residual ε_{ijk} is derived from the following ratios with $n = n_i n_j n_k$:

$$\hat{R}^2_\alpha = \frac{SS_\alpha - (n_i - 1)\, \frac{SS_\varepsilon}{n - n_i n_k}}{SS_t} \tag{12}$$

$$\hat{R}^2_\beta = \frac{SS_\beta - (n_k - 1)\, \frac{SS_\varepsilon}{n - n_i n_k}}{SS_t} \tag{13}$$

$$\hat{R}^2_\gamma = \frac{SS_\gamma - (n_i - 1)\,(n_k - 1)\, \frac{SS_\varepsilon}{n - n_i n_k}}{SS_t} \tag{14}$$

$$\hat{R}^2_\varepsilon = \frac{\frac{n-1}{n - n_i n_k} SS_\varepsilon}{SS_t} \tag{15}$$

The individual portions of explained variance in eqs (12)–(15) are Fisher F distributed under the Nullhypothesis with appropriately chosen degrees of freedom. The method can also be applied when the time series in X are lowpass filtered. In this study, we apply a running-mean lowpass filter with stepwise increasing filter length between 1 and 30 yr to remove variability from X below a certain time scale and to assess to what extent the common climate change signal β_k prevails at that time scale. When applying this spectral approach the degrees of freedom have been adjusted to each time scale by estimating the autocorrelation function of the lowpass filtered index time series.

3. Observed and simulated changes

The observed interdecadal variations of the four considered circulation modes—NPI, NAO, NAM and SAM—are illustrated in Fig. 1 during the time period 1949–2008. Variability at time scales shorter than 11 yr has been removed by a running-mean lowpass filter to focus on the long-term changes presumably induced by increasing GHG concentrations (Deser and Phillips, 2009). The NPI time series is characterized by a slightly negative trend, equivalent to a strengthening of the Aleutian low. The observed variations are inside the range spanned by 56 individual 20th-century model simulations and, hence, can be conceived as one realization covered by the multi-model ensemble. The multi-model mean time series, however, is uncorrelated to the observations. The NAO index reveals a clear positive trend which is also occurring in the multi-model mean time series, albeit of much lower amplitude. The same is true for the NAM and SAM. In particular, the SAM trend from HadSLPr is outstanding. It is often referred to as one of the presumed most robust and striking indicators of anthropogenic climate change (Cai et al., 2005). The station-based SAM index from Marshall (2003) is not subject to a comparable trend component, however, it is closer to the amplitude of the multi-model ensemble mean time series. The NAO and NAM time series have undergone a noticeable decline between 1996 and 2004 which has been interpreted as the effect of internal variability superimposed on a GHG-induced long-term trend (Overland and Wang, 2005),

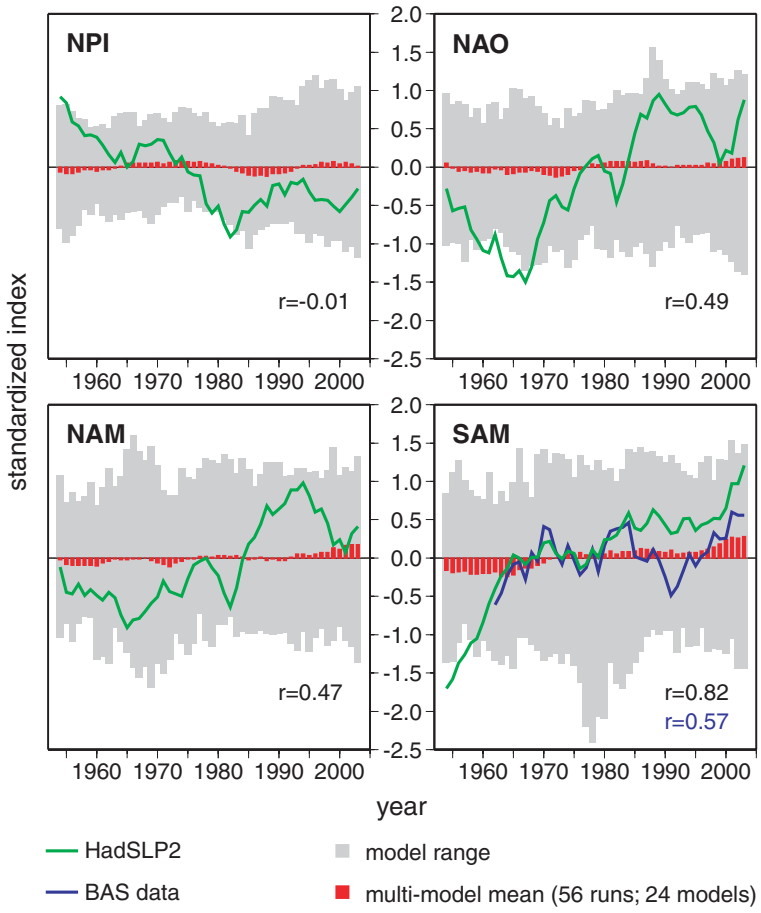

Fig. 1. Observed and multi-model mean 11-year lowpass filtered time series of the North Pacific Index (NPI), the North Atlantic Oscillation (NAO), the Northern (NAM) and Southern (SAM) Annular Modes in winter during the 1949–2008 period. The observed time series refer to the Hadley Centre SLP data set. The range over 56 model runs from 24 climate models is marked grey. The multi-model mean time series are plotted as red bars. For SAM, the station-based SAM index according to the British Antarctic Survey (BAS; Marshall, 2003) is plotted as well. The indicated correlation coefficients (r) are statistically significant at the 10% level except for NPI.

although man-made radiative forcing is presently twice as much as in the 1970s and 1980s.

The multi-model mean during the 20th century is in phase with the observed interdecadal variability but systematically underestimates the amplitudes by a factor of 10. This cannot entirely be explained by the multi-model ensemble averaging because the observed NAM and SAM time series partly exceed the range of individual model simulations. The amplitude error represents a major deficiency of state-of-the-art climate models which probably arises from missing feedbacks and teleconnections in the models, like for instance with stratospheric and sea-ice dynamics (Gillett and Thompson, 2003; Rind et al., 2005a,b). Therefore, it cannot be ruled out that the yet quite impressive simulated trends in the 21st century are still underestimated.

The multi-model mean time series until the end of the 21st century are a clear function of circulation mode and imposed emission scenario (Fig. 2). For comparison all model time series are normalized to the observational period 1949–2008. According to the observed trends, the SAM is characterized by the most pronounced strengthening. On average over 53 simulations from 24 models the shift amounts to more than 1.5 standard deviations towards a more positive mean state under the intermediate A1B emission scenario. Under the B1 mitigation scenario the change is in the order of +1 standard deviation, under the business-as-usual scenario A2 beyond +2 standard deviations. In the face of multi-model ensemble averaging such a shift is indeed enormous. The temporal evolution of the NAO and NAM time series is similar at the decadal time scale. However, the NAM is found to be more sensitive to the radiative heating, at least in the multi-model ensemble mean. The reason is that the NAM index captures the decrease of SLP over the northern polar cap which is a common feature to most climate models, while the NAO index is confined to the centres of action in the North Atlantic (Rauthe et al., 2004; Miller et al., 2006; Stephenson et al., 2006). A weak negative tendency is projected for the NPI which implies an intensification of the Aleutian low, in agreement with the observations (cf. Fig. 1 as well as Hurrell and van Loon, 1997).

The simulated changes in the circulation modes imply a variety of regional climate changes and impacts in the densely populated midlatitudes: a strengthening of the NPI, NAO, NAM and SAM is accompanied by a more zonal structure of the atmospheric flow and the advection of warm and humid air masses in winter from the oceans towards extratropical continents. In the

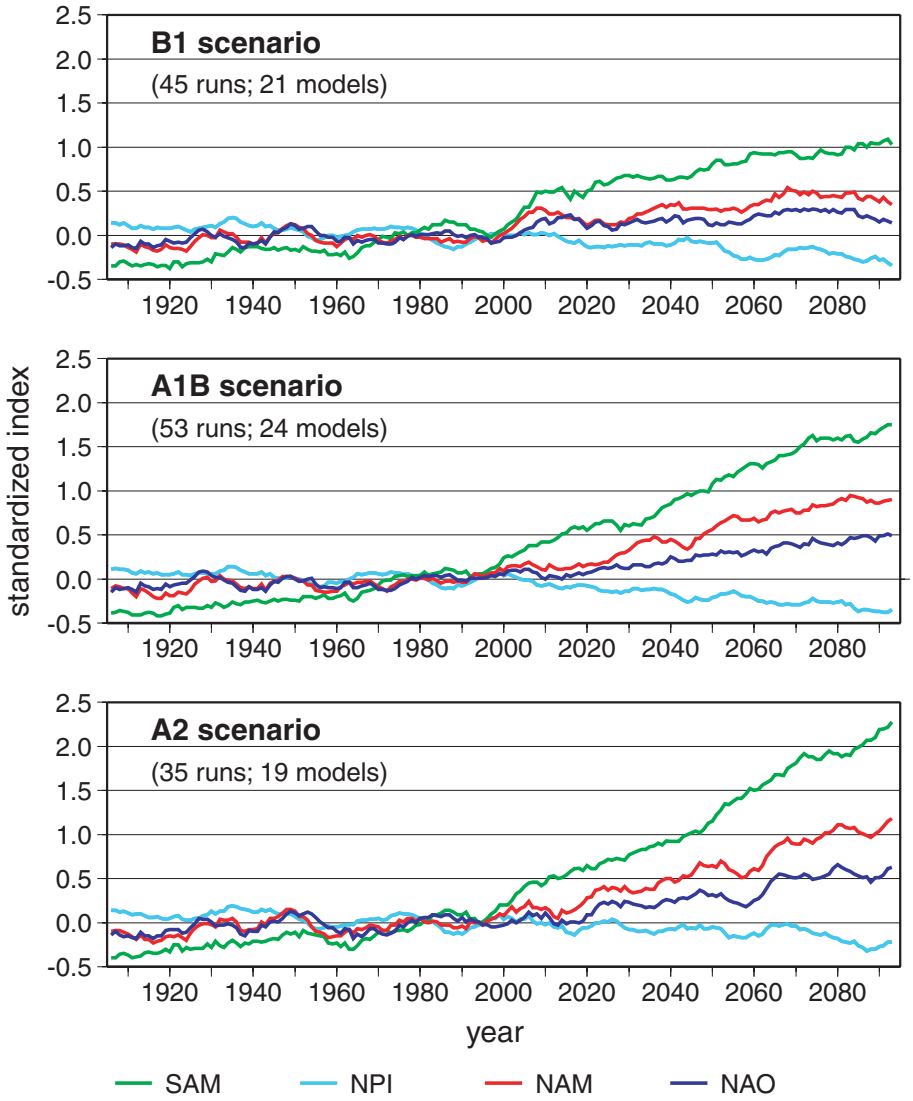

Fig. 2. Projections of the 11-year lowpass filtered multi-model mean time series (not inflated) for the circulation modes shown in Fig. 1 under enhanced radiative forcing until the year 2098 for three emission scenarios from B1 (mitigation policy) to A2 (business as usual). The underlying number of model runs and climate models is indicated.

Southern Hemisphere, the western Antarctic and the Antarctic Peninsula are most affected. On the eastern sides of the Northern Hemisphere land masses cold air advection prevails.

4. Signal analysis

From the simulated changes in Fig. 2 the conclusion may be drawn that the evidence for a future intensification of extratropical circulation modes is high. However, the multi-model mean time series do not reveal the level of uncertainty arising from model differences and the amount of internal variability in the decadal variations of each circulation mode. When results from climate model projections shall be used in decision processes such as adaptation and protection measures, the quality of the climate change signals has to be assessed accurately. In Fig. 3 the SAM time series are plotted for each of the 24 climate models as an example of the remarkable model spread. Although qualitatively all models tend to simulate a strengthening of the SAM until the year 2100—except for GISS-AOM—the amplitude is noticeably different, ranging between +0.5 and +3.0 standard deviations. For the other circulation modes the model spread is still larger and differs even qualitatively. Differences between individual model projections arise from a number of model specifications such as horizontal and vertical resolution, physical parameterizations, considered feedback mechanisms, initial conditions, variable boundary conditions like, for example ozone and aerosol treatment, and partly even the dynamical

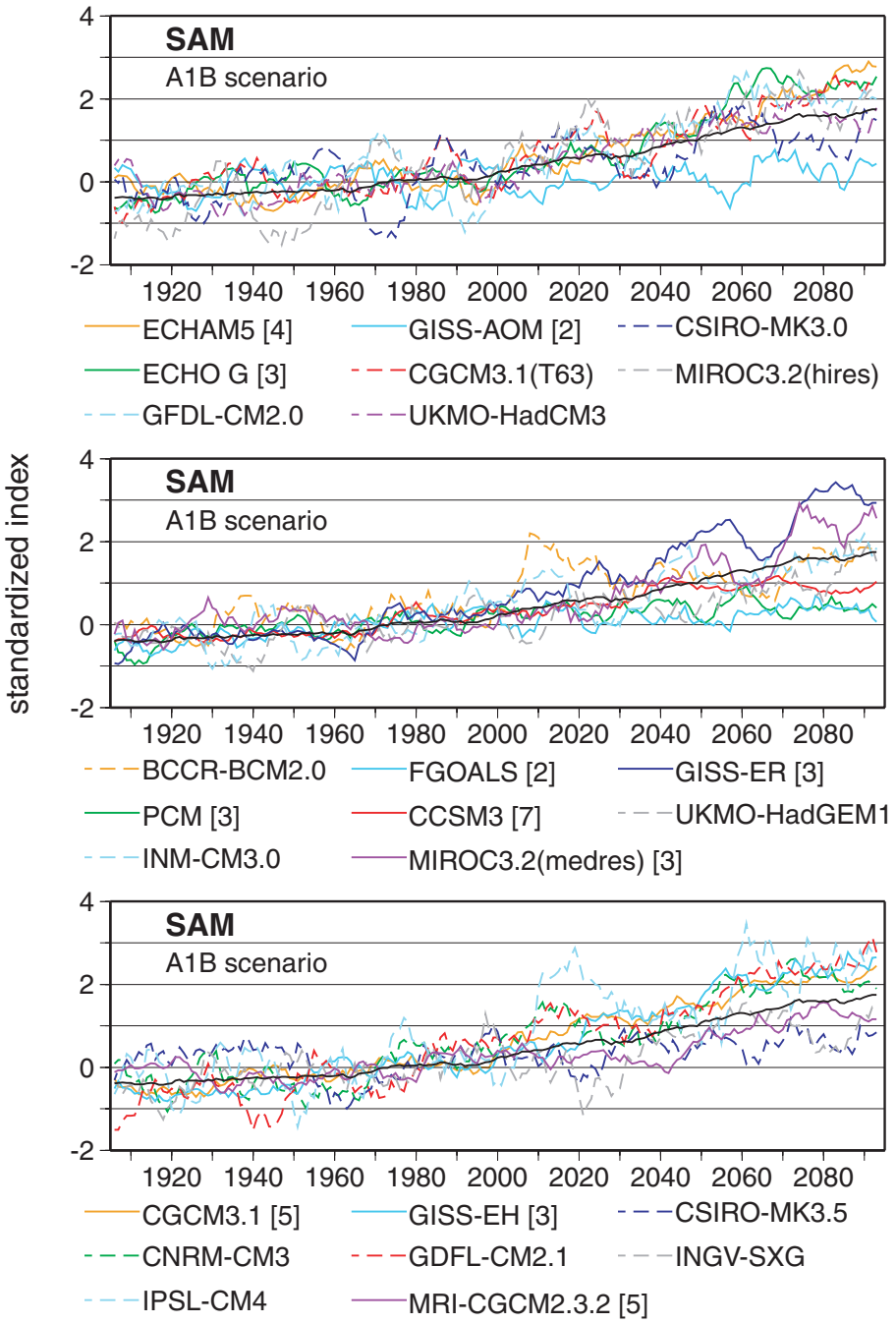

Fig. 3. Projections of the 11-year lowpass filtered SAM time series for all available models under the A1B senario, ensemble means and individual runs, respectively. Numbers in brackets indicate the ensemble size.

core of the model. In the first step of the signal analysis, these model specifications are equally treated as sources of model uncertainty. Hence, all available ensemble simulations are put together under one of the three emission scenarios. In the second step, the multi-model ensemble is further differentiated according to the ozone forcing agent and the models' TOA (Section 5).

Given the large model spread, it is obvious that the signal-to-noise ratio has to be assessed rather than interpreting the multi-model mean trends in Fig. 2. Therefore, we quantify and test the portion of variance in each circulation mode related to anthropogenic radiative forcing and compare this with a quantitative measure of model uncertainty, internal variability and different time responses in the multi-model ensemble. The method is

based on a square-sum decomposition of the total variance using a linear statistical model (Section 2). In addition, the method is combined with a spectral approach to identify the major time scale of predictability arising from anthropogenic radiative forcing.

The results of the spectral signal analysis, applied to all available ensemble simulations under the A1B scenario, are summarized in Fig. 4. In this analysis, it is not differentiated between model simulations with different stratospheric ozone treatment. Although the multi-model ensemble mean time series of the NPI is characterized by a systematic negative tendency (Fig. 2), the effect of anthropogenic radiative forcing takes a back seat compared with the remarkable amount of model uncertainty. Model-dependent differences in the time response, that is the timing and amplitude of climate change, range in the same order of magnitude as the human impact. This result is independent of the considered time scale. For instance, 68% of the total 30-year variations of the NPI in the 40-member multi-model ensemble arise from systematic differences between climate models, 2% are due to anthropogenic radiative forcing, 3% are related to different time responses and 27% can be explained by internal variability. In other words, the strengthening of the Aleutian low in the multi-model ensemble mean is blurred by model uncertainty and, hence, does not represent a robust climate change signal. In terms of the NAO, the greenhouse forcing is somewhat stronger (∼10%) and model uncertainty is below 30%. Instead, internal variability in the coupled climate system is much more pronounced. This finding is not unexpected in a region of frequent cyclo-genesis and—besides the weakening of the Atlantic Meridional Overturning Circulation—may serve as an explanation for the fact that the future warming patterns displayed in the 4th Assessment Report of the IPCC have a minimum in the North Atlantic region (IPCC, 2007a). For the NAM and, even more, the SAM the situation is different: the impact of anthropogenic radiative heating is clearly prevailing, accounting for 25 to 38% of total interdecadal variability, and thus reaches or exceeds the level of model uncertainty. Based on these quantitative estimates an important conclusion can be drawn: under the A1B emission scenario various global climate model simulations disclose a robust climate change signal in the NAM and SAM time series until 2098 which will affect regional climate in large parts of the extratropics. Another conclusion of practical relevance is that the greenhouse forcing leads to predictability at time scales of 10 yr already, whereas higher-frequency variations arise from internal variability in the coupled climate system.

To assess the potential of mitigation policy in terms of future circulation changes the signal analysis is applied to three different emission scenarios, according to the 4th Assessment Report of the Intergovernmental Panel on Climate Change (IPCC) (Meehl et al., 2007). The A2 scenario is a so-called

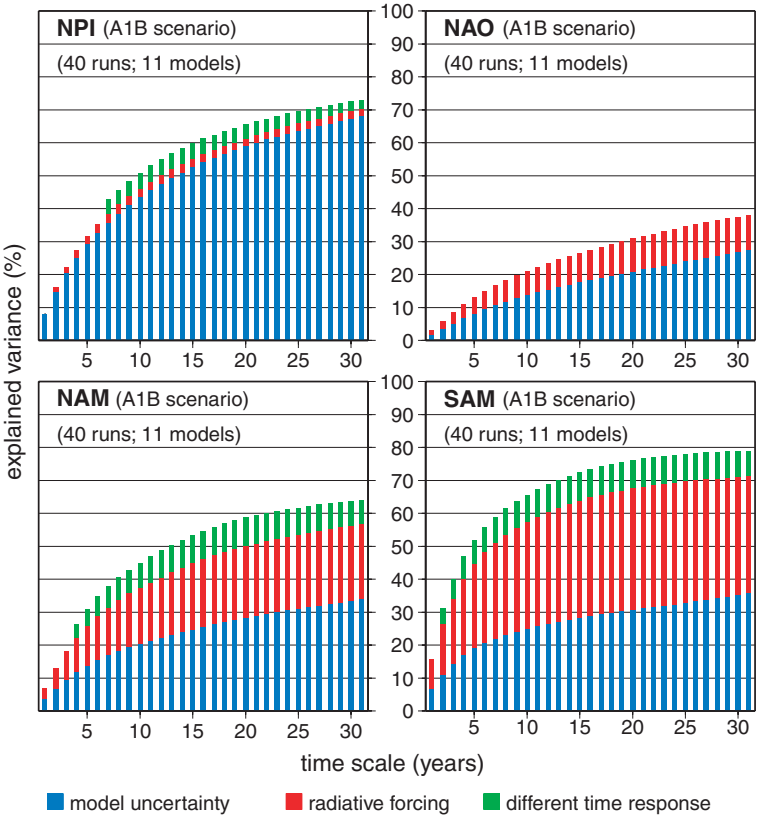

Fig. 4. Portion of variance related to model uncertainty, to anthropogenic radiative forcing according to scenario A1B (including simulations with different stratospheric ozone treatment) and to differences in the time response during the 1970–2098 period for the circulation modes shown in Fig. 1 and for different time scales between 1 and 31 yr. The complementary percentage up to 100% is related to internal variability. The underlying number of model runs and climate models is indicated. Only values statistically significant at the 1% level are displayed.

business-as-usual scenario with prevailing fossil fuel consumption, high demographic growth and regionally divergent development (Nakicenovic and Swart, 2000). This scenario ends up with a CO_2 concentration of around 840 ppm in the year 2100 compared with 280 ppm in the pre-industrial era. A1B is an intermediate scenario assuming a mixture of fossil fuel consumption and extended usage of renewable energy in the future. The 2100 CO_2 concentration amounts to 700 ppm. A successful mitigation policy and positive regional development are assumed in the B1 scenario which leads to 540 ppm until the end of the 21st century. The differences of the climate change signals between the B1 and A2 scenario are illustrated in Fig. 5 for the NAO and SAM index. While the greenhouse forcing under the A2 scenario almost outperforms the level of model uncertainty in terms of the NAO, the climate change signal virtually disappears under the B1 scenario. With respect to the SAM, the spectral signal analysis identifies the same level of model uncertainty under B1 as under A1B but a noticeably lower contribution from anthropogenic radiative forcing, amounting to 20% at the interdecadal time scale. In contrast, the human impact on the SAM rises to 60% of total variance under the A2 scenario. An adequate scenario dependence is found for the NAM. Combined with the different responses in the multi-model ensemble mean time series (for SAM +2.3 versus +1.1 standard deviations towards a more positive mean state until the end of the 21st century, Fig. 2) this scenario intercomparison foreshadows a promising potential of climate mitigation policy in terms of curtailing the amount of future circulation changes. In this respect, the stabilization of climate below a certain maximum shift of the extratropical circulation modes may also be issued as a target for climate protection policy beside the +2 °C guideline (IPCC, 2007b).

5. Ozone and TOA effects

The signal analysis in Section 4 has revealed that model uncertainty is an important aspect of climate change detection. The question is to what extent model uncertainty is unavoidable because some model parameterizations cannot be further improved and, hence, should not be homogenized from model to model, and to what extent model uncertainty arises from model differences which can be homogenized like for instance improved scenarios, feedback processes and resolution. In terms of the extratropical circulation modes, a basic inhomogeneity in the AR4 multi-model ensemble is that the stratospheric ozone forcing agent is treated differently from model to model (cf. Table 1). Some models account for an ongoing stratospheric ozone recovery from the year 2000 onward as a reponse to the Montreal process, some models keep the ozone concentration constant at low-ozone year 2000 conditions with an imposed seasonal cycle, and some models have no specified ozone forcing agent

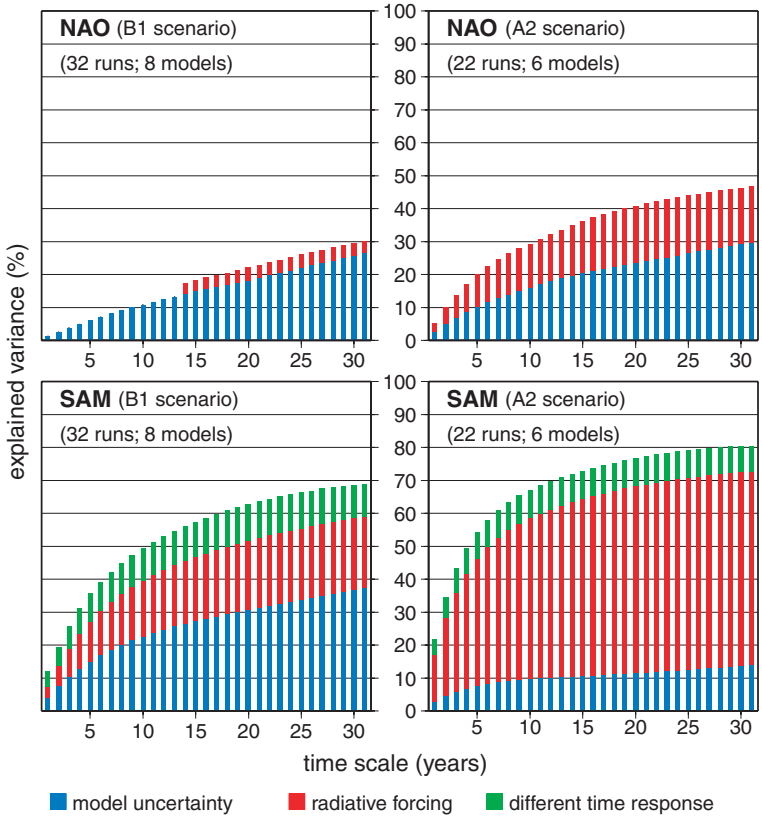

Fig. 5. As Fig. 4 but for NAO and SAM under the B1 and A2 scenario (each including simulations with different stratospheric ozone treatment).

with concentrations held constant at pre-industrial level (Miller et al., 2006; Meehl et al., 2007). In particular, the SAM is sensitive to the stratospheric ozone forcing. Thompson and Solomon (2002) have shown that the strongest observed positive SAM trend has prevailed in austral summer when ozone depletion has led to substantial stratospheric cooling during the second half of the 20th century. This finding is corroborated by climate model simulations for the 20th century (Gillett and Thompson, 2003). Accordingly, climate model projections with ozone recovery simulate a negative SAM trend in summer, in contrast to the positive trend in models without ozone recovery (Perlwitz et al., 2008). The ozone effect on the summer SAM is even larger in coupled chemistry-climate models (Son et al., 2008). In austral winter, the SAM trend appears to be less sensitive to the ozone forcing (Miller et al., 2006; Perlwitz et al., 2008; Son et al., 2008). In the Northern Hemisphere, the positive NAM and NAO trends are reduced in the future when interactive stratospheric ozone is implemented in the ECHO-G climate model (Brand et al., 2008).

To evaluate whether the available AR4 models with different stratospheric ozone forcing significantly differ from each other, we have subdivided the multi-model ensemble into three sub-groups per scenario according to Table 1 and computed the mean changes in the NAM and SAM for each sub-group. For the A1B scenario, the results are shown in Fig. 6. Statistical significance is determined by a *t*-test deriving the standard error from the model deviations before 1970 when ozone forcing has not yet started. In particular, the sub-group with ozone depletion in the 20th and subsequent low ozone concentration systematically differs from the overall multi-model ensemble mean. According to Thompson and Solomon (2002), the positive NAM and SAM trends are significantly intensified. Note that this sub-group is only built by simulations with the GISS climate models (cf. Table 1). Thus, intermodel variability may be considerably lower than in the other sub-groups. Simulations with 21st-century ozone recovery during summer are largely consistent with the multi-model ensemble mean, whereas projections with pre-industrial ozone level reveal weaker positive trends. For the

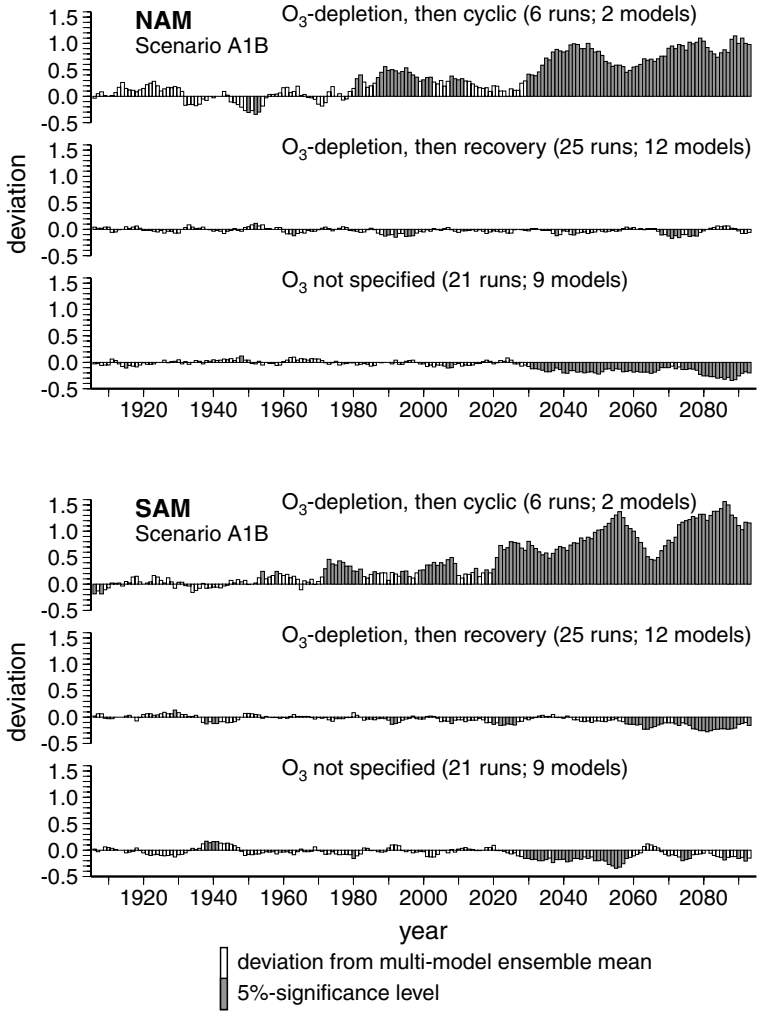

Fig. 6. Deviations of three sub-ensembles with different stratospheric ozone treatment from the multi-model ensemble mean for 11-year lowpass filtered time series of the NAM and SAM under the A1B scenario. Filled bars indicate statistical significance at the 5% level. See text for further explanation.

SAM, this has also been reported by Perlwitz et al. (2008) as well as Son et al. (2008) and is in complete contrast to the reduced SAM trends in austral summer when ozone recovers after 2000. Obviously, ozone depletion is an important aggravating factor for the SAM and NAM trends in winter by intensifying the meridional temperature gradient between low latitudes and polar caps. Ozone recovery in the 21st century has a positive effect in terms of climate change mitigation in the polar regions but does not reach the level of low circulation changes as given under pre-industrial ozone concentrations. The reason probably is that 21st-century ozone recovery is not reaching the pre-industrial level before around 2085. In the meantime, the lower stratospheric ozone concentration enhances the circulation trends. Another hypothetical explanation may be that ozone recovery in summer leads to specific meridional temperature gradients which persist until the winter season and affect the winter SAM—a matter of ongoing scientific debate. Although no final theory can yet be given for the impact of stratospheric ozone forcing, it is obvious that studies on multi-model climate change signals from AR4 have to account for this basic inhomogeneity, because other climatic processes and variables may also be sensitive to the treatment of the stratospheric ozone agent.

The dynamics of extratropical circulation is also tied to the models' vertical resolution and TOA as key factors for the models' ability to simulate the stratospheric circulation and sudden warmings, although the picture is not yet clear: Shindell et al. (1999) have pointed to the necessity of enhanced vertical resolution and TOA to reproduce the observed prominent NAM trend in the late 20th century. In contrast, Huebener et al. (2007) suggest a weakening of the NAM trend in their coupled troposphere–stratosphere model, whereas Gillett et al. (2002) find no sensitivity of the NAM dynamics to the models' TOA. Dall'Amico et al. (2009) highlight the importance of stratospheric internal variability, long-term trends as well as the quasi-biennial oscillation (QBO) to reproduce the observed development of the SAM in the late 20th century. The same is reported by Scaife et al. (2005) with respect to the recent NAM trend.

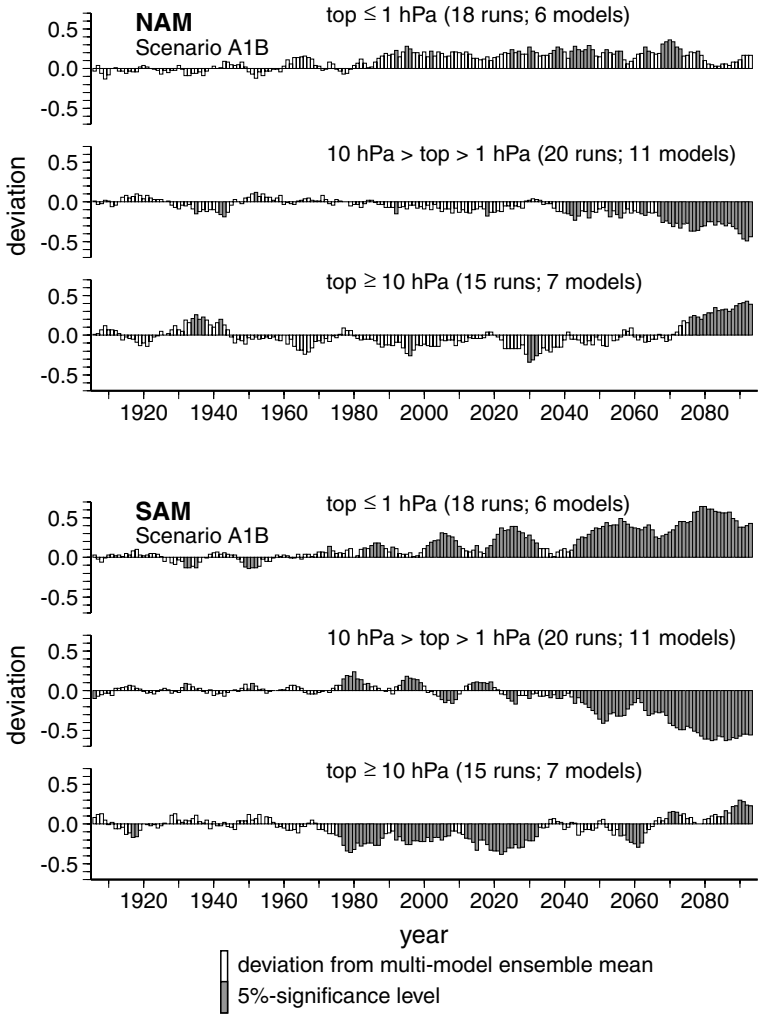

Fig. 7. Same as Fig. 6 but for three sub-ensembles grouped according to the models' top-of-the-atmosphere, using 10 hPa as lower and 1 hPa as upper threshold.

Within the AR4 multi-model ensemble the vertical resolution does not vary considerably from climate model to climate model (IPCC, 2007a). Therefore, the data set can be regarded as homogeneous in this respect. However, the models' TOA is in the range between 15 and 0.05 hPa (cf. Table 1). To assess the sensitivity of the NAM and SAM trends to the TOA, the AR4 data set is split up into three sub-groups per scenario with 10 hPa as lower and 1 hPa as upper threshold. These categories lead to sub-samples of comparable size. The deviations of each sub-group from the multi-model ensemble mean is displayed in Fig. 7 for the A1B scenario. Again, the standard error under the Nullhypothesis is taken from the deviations prior to 2000, assuming that the greenhouse forcing mainly prevails in the 21st century. Although the climate model projections with highest TOA are characterized by the strongest SAM trend, the overall picture is not coherent: in the intermediate group the SAM trend is significantly lower than in the group with TOA $\geq$ 10 hPa and no systematic effect is found for the NAM. Thus, the climate change signals in Section 4 obviously are not affected by this feature. Note that this does not imply that the AR4 multi-model ensemble is correct in terms of the presentation of stratospheric dynamics and related circulation responses. It is also conceivable that all models are deficient in this respect. Therefore, the subsequent AR5 modelling initiative should rely on climate model simulations with enhanced vertical resolution and TOA, in combination with reasonable scenarios of ozone forcing in the 21st century.

6. Conclusions

Based on the AR4 multi-model ensemble, our study has revealed prominent changes in the major extratropical circulation modes until the end of the 21st century which are basically consistent with the observed intensification since the 1970s. Although the model spread is still quite high, climate change signals could be identified for the SAM and NAM which stand out from model uncertainty and internal model variability at time scales from 10 yr onward. Climate protection policy as represented by the B1 emission scenario has a clear mitigating effect on the climate change signals. The circulation trends significantly differ between model projections with and without stratospheric ozone depletion. In contrast, the models' TOA has no systematic impact within the AR4 multi-model ensemble.

Based on the signal analysis, an important conclusion can be drawn: under the A1B and, in particular, the A2 emission scenario various global climate model simulations disclose a robust climate change signal in the NAM and SAM time series until 2098 which will affect regional climate in large parts of the extratropics. Another conclusion of practical relevance is that the greenhouse forcing leads to some predictability, at least of the SAM, at time scales of 10 yr already, whereas higher-frequency variations arise from internal variability in the coupled climate system. The scenario intercomparison foreshadows a promising potential of climate mitigation policy with positive implications for regional climate change. In this context, it would be interesting to assess what level of extratropical circulation changes can be achieved under the greenhouse gas emissions which are allowed in the framework of the $+2\,^{\circ}$C benchmark (IPCC, 2007b).

Although it is an advancement that state-of-the-art climate models produce robust climate change signals which can be used as predictors of regional climate impacts, a basic caveat still is that the sensitivity of atmospheric circulation to radiative forcing may be underestimated—or overestimated—by present-day climate models because important feedbacks and climate system components are not incorporated or resolved in all models (cf. Gillett and Thompson, 2003; Rind et al., 2005a,b). The different treatments of the stratospheric ozone forcing agent is one example for a basic inhomogeneity within the AR4 multi-model ensemble—a matter for model improvements in preparation of the 5th Assessment Report of the IPCC.

7. Acknowledgments

The authors thank the Hadley Centre for providing the HadSLPr data set and the British Antarctic Survey for making available the station-based SAM index. Furthermore, the authors acknowledge the modelling groups, the Program for Climate Model Diagnosis and Intercomparison (PCMDI) and the WCRP's Working Group on Coupled Modelling (WGCM) for their roles in making available the WCRP CMIP3 multi-model dataset. Support of this data set is provided by the Office of Science, U.S. Department of Energy. Finally, the authors are grateful for the helpful and constructive comments by two anonymous reviewers.

References

Allan, R. and Ansell, T. 2006. A New Globally Complete Monthly Historical Gridded Mean Sea Level Pressure Dataset (HadSLP2): 1850–2004. *J. Clim.* **19**, 5816–5842.

Brand, S., Dethloff, K. and Handorf, D. 2008. Tropospheric circulation sensitivity to an interactive stratosphere. *Geophys. Res. Lett.* **35**, doi:10.1029/2007GL032312.

Cai, W., Shi, G., Cowan, T., Bi, D. and Ribbe, J. 2005. The response of the southern annular mode, the East Australien current, and the southern mid-latitude ocean circulation to global warming. *Geophys. Res. Lett.* **32**, doi:10.1029/2005GL024701.

Dall'Amico, M., Stott, P. A., Scaife, A. A., Gray, L. J., Roselof, K. H. and co-authors. 2009. Impact of stratospheric variability on tropospheric climate change. *Clim. Dyn.*, doi:10.1007/s00382-009-0580-1.

Deser, C. and Phillips, A. S. 2009. Atmospheric circulation trends, 1950-2000: The relative roles of sea surface temperature forcing and direct atmospheric radiative forcing. *J. Clim.* **22**, 396–413.

Gillett, N. P. and Thompson, D. W. J. 2003. Simulation of recent southern hemisphere climate change. *Science* **302**, 273–275.

Gillett, N. P., Allen, M. R., McDonald, R., Senior, C. A., Shindell, D. T. and co-authors. 2002. How linear is the Arctic Oscillation response to greenhouse gases? *J. Geophys. Res.* **17**, doi:10.1029/2001JD000589.

Gong, D. and Wang, S. 1999. Definition of Antarctic oscillation index. *Geophys. Res. Lett.* **26**, 459–462.

Gouveia, C., Trigo, R. M., DaCamara, C. C., Libonati, R. and Pereira, J. M. C. 2008. The North Atlantic Oscillation and European vegetation dynamics. *Int. J. Climatol.* **28**, 1835–1847.

Hallett, T. B., Coulson, T., Pilkington, J. G., Clutton-Brock, T. H., Pemberton, J. M. and co-authors. 2004. Why large-scale climate indices seem to predict ecological processes better than local weather.*Nature* **430**, 71–75.

Huebener, H., Cubasch, U., Langemaatz, U., Spangehl, T., Niehorster, F. and co-authors. 2007. Ensemble climate simulation using a fully coupled ocean-troposphere-stratosphere general circulation model. *Phil. Trans. R. Soc. A.* **365**, 2089–2101.

Hurrell, J. W. 1995. Decadal trends in the North Atlantic Oscillation: regional temperatures and precipitation. *Science* **269**, 676–679.

Hurrell, J. W. and van Loon, H. 1997. Decadal variations in climate associated with the North Atlantic Oscillation. *Clim. Change* **36**, 301–326.

Hurrell, J. W., Visbeck, M., Busalacchi, A., Clarke, R. A., Delworth, T. L. and co-authors. 2006. Atlantic climate variability and predictability: a CLIVAR perspective. *J. Clim.* **19**, 5100–5121.

IPCC 2007a. Climate Change 2007: The Physical Science Basis. In: *Contribution of working group I to the fourth Assessment Report of the Intergovernmental Panel on Climate Change*, (eds. S. Solomon, D. Qin, M. Manning, Z. Chen, M. Marquis, K. B. Averyt, M. Tignor and H. L. Miller). Cambridge University Press, Cambridge, UK and New York, NY, USA, 996.

IPCC 2007b. Climate Change 2007: Mitigation of Climate Change. In: *Contribution of working group III to the fourth Assessment Report of the Intergovernmental Panel on Climate Change*, (eds. B. Metz, O. Davidson, P. Bosch, R. Dave and L. Meyer). Cambridge University Press, Cambridge, UK and New York, NY, USA, 851.

IPCC 2007c. Climate Change 2007: Impacts, Adaptation and Vulnerability. In: *Contribution of working group II to the fourth Assessment Report of the Intergovernmental Panel on Climate Change*, (eds. M. L. Parry, O. F. Canziani, J. P., Palutikof, P. J. van der Linden and C. E. Hanson). Cambridge University Press, Cambridge, UK, 976.

Kuzmina, S. I., Bengtsson, L., Johannessen, O. M., Drange, H., Bobylev, L. P. and co-authors. 2005. The North Atlantic Oscillation and greenhouse-gas forcing. *Geophys. Res. Lett.* **32**, doi:10.1029/2004GL021064.

Lubin, D., Wittemyer, R., Bromwich, D. and Marshall, G. 2008. Antarctic Peninsula mesoscale cyclone variability and climatic impacts influenced by the SAM. *Geophys. Res. Lett.* **35**, doi:10.1029/2007GL032170.

Meehl, G. A., Covey, C., Delworth, T., Latif, M., McAvaney, B. and co-authors. 2007. The WCRP CMIP3 Multimodel Dataset: A New Era in Climate Change Research. *Bull. Am. Meteorol. Soc.* **88**, 1383–1394.

Marshall, G. J. 2003. Trends in the Southern annular mode from observations and reanalyses. *J. Clim.* **16**, 4134–4143.

Miller, R. L., Smith, G. A. and Shindell, D. T. 2006. Forced annular variations in the 20th century Intergovernmental Panel on Climate Change fourth Assessment Report models. *J. Geophys. Res.* **111**, doi:10.1029/2005JD006323.

Min, S.-K. and Hense, A. 2006. A Bayesian approach to climate model evaluation and multi-model averaging with an application to global mean surface temperatures from IPCC AR4 coupled climate models. *Geophys. Res. Lett.* **33**, doi:10.1029/2006GL 025779.

Mo, K. C. 2000. Relationships between low-frequency variability in the southern hemisphere and sea surface temperature anomalies. *J. Clim.* **13**, 3599–3610.

Nakicenovic, N. and Swart, R. (eds.) 2000. Emission scenarios 2000. *Special Report of the Intergovernmental Panel on Climate Change*. Cambridge University Press, Cambridge.

Overland, J. E. and Wang, M. 2005. The Arctic paradox: the recent decrease of the Arctic Oscillation. *Geophys. Res. Lett.* **32**, doi:10.1029/2004GL021752.

Paeth, H. and Hense, A. 2002. Sensitivity of climate change signals deduced from multi-model Monte Carlo experiments. *Clim. Res.* **22**, 189–204.

Paeth, H. and Hense, A. 2004. SST versus climate change signals in West African rainfall: 20th century variations and future projections. *Clim. Change* **65**, 179–208.

Paeth, H., Rauthe, M. and Min, S.-K. 2008. Multi-model Bayesian assessment of climate change in the northern annular mode. *Global Planet. Change* **60**, 193–206.

Perlwitz, J., Pawson, S., Fogt, R. L., Nielsen, J. E. and Neff, W. D. 2008. Impact of stratospheric ozone hole recovery on Antarctic climate. *Geophys. Res. Lett.* **35**, doi:10.1029/2008GL033317.

Quadrelli, R. and Wallace, J. M. 2004. A simplified linear framework for interpreting patterns of Northern Hemisphere wintertime climate variability. *J. Clim.* **17**, 3728–3744.

Rauthe, M. and Paeth, H. 2004. Relative importance of Northern Hemisphere circulation modes in predicting regional climate change. *J. Clim.* **17**, 4180–4189.

Rauthe, M., Hense, A. and Paeth, H. 2004. A model intercomparison study of climate change signals in extratropical circulation. *Int. J. Climatol.* **24**, 643–662.

Rind, D., Perlwitz, J. and Lonergan, P. 2005a. AO/NAO response to climate change: 1. Respective influences of stratospheric and tropospheric climate changes. *J. Geophys. Res.* **110**, doi:10.1029/2004JD005103.

Rind, D., Perlwitz, J., Lonergan, P. and Lerner, J. 2005b. AO/NAO response to climate change: 2. Relative importance of low- and high-latitude temperature changes. *J. Geophys. Res.* **110**, doi:10.1029/2004JD005686.

Scaife, A. A., Knight, J. R., Vallis, G. K. and Folland, C. K. 2005. A stratospheric influence on the winter NAO and North Atlantic surface climate. *Geophys. Res. Lett.* **32**, doi:10.1029/2005GL023226.

Semenov, V. A., Latif, M., Jungclaus, J. H. and Park, W. 2008. Is the observed NAO variability during the instrumental record unusual? *Geophys. Res. Lett.* **35**, doi:10.1029/ 2008GL033273.

Shindell, D. T., Miller, R. L., Schmidt, G. A. and Pandolofs, L. 1999. Simulation of recent northern climate trends by greenhouse-gas forcing. *Nature* **399**, 452–455.

Son, S. W., Polvani, L. M., Waugh, D. W., Akiyoshi, H., Garcia, R. and co-authors. 2008. The Impact of stratospheric ozone depletion on the southern hemisphere westerly jet. *Science* **320**, 1486–1489.

Stephenson, D. B. and Pavan, V. 2003. The North Atlantic Oscillation in coupled climate models: a CMIP1 evaluation. *Clim. Dyn.* **20**, 381–399.

Stephenson, D. B., Pavan, V., Collins, M., Junge, M. M., Quadrelli, R., and Participating CMIP2 Modelling Groups 2006. North Atlantic Oscillation response to transient greenhouse gas forcing and the impact

on European winter climate: a CMIP2 multi-model assessment. *Clim. Dyn.* **27**, 401–420.

Tebaldi, C., Smith, R. L., Nychka, D. and Mearns, L. O. 2005. Quantifying uncertainty in projections of regional climate change: a Bayesian approach to the analysis of multimodel ensembles. *J. Clim.* **18**, 1524–1540.

Thompson, D. W. J. and Solomon, S. 2002. Interpretation of recent southern hemisphere climate change. *Science* **296**, 895–899.

Thompson, D. W. J. and Wallace, J. M. 2001. Regional climate impacts of the northern hemisphere annular mode. *Science* **293**, 85–89.

Ulbrich, U. and Christoph, M. 1999. A shift of the NAO and increasing strom track activity over Europe due to anthropogenic greenhouse gas forcing. *Clim. Dyn.* **15**, 551–559.

Ulbrich, U., Pinto, J. G., Kupfer, H., Leckebusch, G. C., Spangehl, T. and co-authors. 2008. Changing Northern Hemisphere strom tracks in an ensemble of IPCC climate change simulations. *J. Clim.* **21**, 1669–1679.

von Storch, H. and Zwiers, F. W., 1999. *Statistical Analysis in Climate Research*. Cambridge University Press, Cambridge, UK and New York, NY, 484.

Wang, X. L. and Swail, V. R. 2006. Climate change signal and uncertainty in projections of ocean wave heights. *Clim. Dyn.* **26**, 109–126.

Wunsch, C. 1999. The interpretation of short climate records, with comments on the North Atlantic and Southern Oscillation. *Bull. Am. Met. Soc.* **80**, 245–255.